Triple silicon isotope insights into the formation of Precambrian cherts

Haoxuan Sun, Marc Chaussidon, François Robert, Shengyu Tian, Zhengbin Deng, Frédéric Moynier

Triple silicon isotope insights into the formation of Precambrian cherts

Haoxuan Sun[a,*], Marc Chaussidon[a], François Robert[b], Shengyu Tian[a], Zhengbin Deng[c], Frédéric Moynier[a]

[a] *Université Paris Cité, Institut de physique du globe de Paris, CNRS, 1 rue Jussieu, Paris 75005, France*

[b] *Institut Origine et Evolution (O&E), Muséum national d'Histoire naturelle et Sorbonne Université, IMPMC-UMR 7590 CNRS, 57 rue Cuvier, Paris 75005, France*

[c] *Centre for Star and Planet Formation, Globe Institute, University of Copenhagen, Copenhagen, Denmark*

**Corresponding author*

Email address: sun@ipgp.fr

Abstract

Cherts are pervasive in the Precambrian and their O and Si isotopic compositions have been used extensively for reconstructing seawater paleo-temperatures. However, these reconstructions are obscured by the fact that cherts exhibit, at a given age, a large isotopic (O and Si) heterogeneity at bulk and micrometer scales. This is understood as reflecting the fact that cherts are an assemblage of silica precursors having different origins, and that diagenesis and metamorphism have modified the isotopic compositions acquired during the last equilibration with seawater. To test the contributions of the different processes that control the Si isotopic composition of cherts, we developed high-precision triple Si isotope measurements by Multicollector-Inductively Coupled-Plasma Mass-Spectrometer (MC-ICP-MS). This approach allows to identify deviations from the equilibrium Si isotopic fractionation at the level of a few ppm. Triple Si isotope data combined with trace elements and O isotope data in Precambrian cherts demonstrate that three different sources of silica were involved in the formation of cherts, and that both equilibrium and kinetic isotopic fractionation took place for Si. Archean seawater is predicted to have a triple Si isotopic composition kinetically fractionated relative to bulk silicate Earth. This requires a large kinetic isotopic fractionation during hydrothermalism of the oceanic crust and appears consistent with warm oceans in the Precambrian. However more work is required on the triple isotope systematics of Si inputs and output to seawater by rivers and authigenic clays formation. Triple Si isotope variations can thus be used as a new tool to unravel the origin of cherts and of their O and Si isotopic compositions. The present evidence of kinetic isotopic fractionations for Si isotopes also implies that Si isotopes should be associated to triple O isotope for paleotemperature reconstructions.

Keywords

Triple silicon isotope, kinetic isotopic fractionation, Precambrian chert, seawater temperature.

1. Introduction

Precambrian cherts are sedimentary rocks composed mainly of microquartz (i.e., micrometer size quartz grains) formed during the diagenetic transformation of sediments rich in amorphous silica and precipitated on the seafloor from seawater (Knauth, 2018). Before the evolution of silica-secreting organisms ~ 500 Ma, seawater was presumably silica-saturated and cherts were consequently abundant among Precambrian marine sediments (Siever, 1992). The oxygen and silicon isotopic composition of cherts constitutes one of the major proxies to reconstruct the evolution of seawater temperature in the Precambrian (Knauth and Lowe, 1978; Robert and Chaussidon, 2006). Precambrian cherts have been shown to display secular systematic mass-dependent variations of oxygen and silicon isotopes ($\delta^{18}O$ and $\delta^{30}Si$, see section 2) with, notably, a depletion of the heavier isotopes of oxygen and silicon in Archean cherts (Knauth and Lowe, 1978; Robert and Chaussidon, 2006). The ~ 15‰ lower $\delta^{18}O$ values of early Archean cherts relative to modern ones have been proposed to reflect seawater temperatures higher by ~ 55 - 85°C (Knauth, 2005 and refs therein). Similarly, the ~ 4‰ $\delta^{30}Si$ variations, positively correlated with variations of $\delta^{18}O$ values, have been shown to be consistent with a change of ~ 50°C of seawater temperature (Robert and Chaussidon, 2006). In this model, the increase of seawater $\delta^{30}Si$ during the Archean results from an increase of the difference between the temperature of hydrothermal fluids leaching the oceanic crust and that of seawater, causing an increase of sequestration of hydrothermal quartz (depleted in ^{30}Si) in the oceanic crust and consequently an increase of the $\delta^{30}Si$ brought to seawater by hydrothermal fluids.

However, a decrease of seawater temperature during the Archean is not the only process which can contributes to the observed increase of seawater $\delta^{30}Si$. Si isotopic studies of rivers have shown that dissolved Si released from the weathering of the continents has in average positive $\delta^{30}Si$ (from 0.2 to 1.5‰ with Yangtze River extremely fractionated up to 3‰; De La Rocha et al., 2000; Ding et al., 2004; Gaspard et al., 2021; Georg et al., 2006). This is due to the fact that ^{30}Si is enriched in water during the formation of secondary minerals such as clays and during the uptake of Si by plants (De La Rocha et al., 1997; Opfergelt et al., 2008; Sun et al., 2016). While in phanerozoic times the Si flux to the oceans from the continents dominated over the hydrothermal flux from the oceanic crust (Tréguer et al., 2021), this would have been very different in the early Archean. An increase of continental versus hydrothermal sources, due to continental growth in the Archean, can contribute to the increase of seawater $\delta^{30}Si$ (Chakrabarti et al., 2012). Another process able to affect the $\delta^{30}Si$ of seawater is the formation of authigenic clays in marine sediments from cations dissolved in pore waters and seawater (or pore waters) Si, i.e. reverse weathering (Trower and Fischer, 2019). While precipitation of amorphous silica from seawater will tend to decrease, by mass balance, seawater $\delta^{30}Si$ (because amorphous silica is likely enriched in ^{30}Si, *Appendix*), the formation of authigenic clays will deplete seawater in ^{30}Si (Oelze et al., 2015; Zheng et al., 2016). An increased flux of Si sequestration by formation of authigenic clays relative to amorphous silica would result in an increased seawater $\delta^{30}Si$ (Trower and Fischer, 2019).

Another limitation of temperature reconstructions based on O and Si isotopes is that they depend on two critical assumptions. First, for reconstructions based on oxygen isotopes, the Precambrian seawater $\delta^{18}O$ must be assumed. Several studies have shown that the $\delta^{18}O$ of seawater was constant at a time scale of 200 - 300 Ma and close to its modern value (Gregory, 2003; Muehlenbachs and Clayton, 1976; Pope et al., 2012; Tartèse et al., 2017; Olson et al., 2022) but this has been challenged by advocating that a secular change took place in the balance between low-temperature and high-temperature fluid/rock interactions in the continental and oceanic crusts (Herwartz, 2021; Jaffrés et al., 2007; Sengupta and Pack, 2018). Second, it must be assumed that the isotope composition of the chert is controlled by isotopic equilibrium with seawater and has not been modified by secondary processes such as hydrothermalism, metamorphism or alteration (Sharp et al., 2016). The validity of this assumption is difficult to test because petrological observations (Knauth, 2018) and in-situ $\delta^{18}O$ and $\delta^{30}Si$ analyses (Marin et al., 2010; Marin-Carbonne et al., 2012) have shown that cherts are actually very complex sedimentary rocks made dominantly of microquartz, but containing also a significant fraction of other forms of silica. Microquartz itself is not a direct precipitate from seawater but results from diagenetic transformations of the sedimentary amorphous silica precursors, at temperatures higher than seawater and with pore fluids that can differ from seawater. Ion microprobe $\delta^{18}O$ and $\delta^{30}Si$ analyses have shown that microquartz is characterized by several permil O and Si isotopic variations at micrometer scale which reflect the process of diagenesis and can be used to quantify the degree of the preservation of cherts (Marin-Carbonne et al., 2014 and refs therein). Back-correcting the effects of diagenesis on the O isotopic composition, allows to better constrain the temperature of seawater with, for instance at 1.9 Ga from microquartz in Gunflint cherts, 30 - 52˚C (Marin et al., 2010), i.e. ~ 15 - 20˚C lower than that calculated from bulk $\delta^{18}O$ values on apparently pure microquartz fractions (Winter and Knauth, 1992).

Recently, improvements in the precision of oxygen isotopic measurements have demonstrated the potential of triple oxygen isotope data in hydrothermal and sedimentary rocks to estimate both the temperature and isotopic composition of the fluid with which the rock last equilibrated (Herwartz et al., 2015; Pack and Herwartz, 2014; Sharp et al., 2016). Triple oxygen isotope studies of Precambrian cherts still come to different conclusions on Precambrian seawater temperatures with either values at around 70 °C (Lowe et al., 2020; McGunnigle et al., 2022) or lower temperatures (Herwartz, 2021). Here we report the first high-precision triple silicon isotopic composition of Precambrian cherts, including a suite of samples from a single ~ 1.5 Ga basin (Jixian cherts) and several Archean cherts between 2.0 and 3.5 Ga. These data demonstrate that the silicon isotopic composition of the various forms of quartz in Archean cherts is the result of a combination of equilibrium and kinetic isotopic fractionations. This brings new constraints on the formation of Archean cherts and on the origin of the secular variations of their Si isotopic composition and has also key potential consequences for seawater temperature reconstruction from O isotopic compositions.

2. Triple silicon isotope systematics

The Si isotopic composition is traditionally reported in delta (δ) notation, which is the per mil deviation from the isotopic ratio of a reference standard:

$$\delta^{i}\mathrm{Si} = \left[\left({}^{i}\mathrm{Si}/{}^{28}\mathrm{Si}\right)_{\mathrm{sample}}/\left({}^{i}\mathrm{Si}/{}^{28}\mathrm{Si}\right)_{\mathrm{standard}} - 1\right] \times 1000 \quad (1)$$

where *i* is the nucleon number of silicon isotopes (29 or 30) and NBS-28 (NIST®RM-8546) is used as the reference standard for Si isotopes. The isotopic fractionation factor (α) between phases A and B is defined as the ratio of the isotopic ratios in the two phases A and B:

$$\alpha^{i}_{\mathrm{A-B}} = \left({}^{i}\mathrm{Si}/{}^{28}\mathrm{Si}\right)_{\mathrm{A}}/\left({}^{i}\mathrm{Si}/{}^{28}\mathrm{Si}\right)_{\mathrm{B}} \quad (2)$$

For an isotopic system with more than one isotopic ratio like silicon, the theory of mass-dependent isotopic fractionation shows that, at first order, fractionation factors are exponentially related:

$$\theta = \ln\left(\alpha^{29/28}_{\mathrm{A-B}}\right) / \ln\left(\alpha^{30/28}_{\mathrm{A-B}}\right) \quad (3)$$

where θ is the fractionation exponent and depends on the atomic masses of isotopes (e.g., Bigeleisen and Mayer, 1947). θ is not a constant (e.g., Young et al., 2022), but its value is always close to the ratio of mass differences among isotopes, i.e., $\theta_{\mathrm{Si}} \approx 0.5$. Consequently, in a 3-isotope diagram (δ^{30}Si versus δ^{29}Si), the isotopic mass-dependent fractionation will approximately follow a straight line with a slope λ of ≈ 0.5:

$$\lim_{\delta \to 0} \theta \approx \lim_{\delta \to 0} \frac{\delta^{29}\mathrm{Si_A} - \delta^{29}\mathrm{Si_B}}{\delta^{30}\mathrm{Si_A} - \delta^{30}\mathrm{Si_B}} \quad (4)$$

However, with improved analytical precision, the facts that θ varies in different processes (equilibrium and kinetic isotopic fractionations) and that the correlation between δ^{29}Si and δ^{30}Si is non-linear (Eq 4) make the bias from the real fractionation line in a 3-isotope diagram non-negligible anymore. Hulston and Thode (1965) firstly recast δ into a logarithmic form notation, delta prime (δ'), to remove this bias:

$$\delta'^{i}\mathrm{Si} = \ln\left[\left({}^{i}\mathrm{Si}/{}^{28}\mathrm{Si}\right)_{\mathrm{sample}}/\left({}^{i}\mathrm{Si}/{}^{28}\mathrm{Si}\right)_{\mathrm{standard}}\right] \times 1000 \quad (5)$$

and a strict linear relationship can be built by using delta prime notation (Miller, 2002):

$$\delta'^{29}\mathrm{Si} = \lambda \times \delta'^{30}\mathrm{Si} + \gamma \quad (6)$$

In the following we use delta prime notation for triple silicon systematics to avoid potential bias, even if this bias would be at the ppm level and, thus, negligible for the present Si isotopic variations in Precambrian cherts.

At high temperature, where the quantum effects are small (Bigeleisen and Mayer, 1947; Young et al., 2002), the maximum value of the equilibrium isotopic fractionation exponent, $\theta_{\mathrm{eq,max}}$, can be simply calculated by:

$$\theta_{\mathrm{eq,max}} = (1/m_{28} - 1/m_{29})/(1/m_{28} - 1/m_{30}) \quad (7)$$

Substituting the mass (^{28}Si: 27.97692649 ± 0.00000022; ^{29}Si: 28.97649468 ± 0.00000022; ^{30}Si: 29.97377018 ± 0.00000022; (Audi and Wapstra, 1993)) into Eq. 7 gives a value of $\theta_{\mathrm{eq,max}}$ = 0.5178. In the case of triple oxygen isotopes, which have been much more studied than triple silicon isotopes, it has been shown that θ_{eq} between quartz and water varies significantly with temperature, decreasing from 0.5305 ($\theta_{\mathrm{eq,max}}$) to a minimum of 0.5237 at 0°C (Sharp et al., 2016). No such study yet exists for triple silicon isotopes but it can be anticipated that the change

of θ_{eq} with temperature will be very small for silicon isotopes because the change of equilibrium $\alpha_{silica-water}$ with temperature is one order of magnitude smaller for Si isotopes (≈1 ‰ for the $^{30}Si/^{28}Si$ ratio between 25 and 75 °C, *Appendix*) than for O isotopes (≈ 11‰ for the $^{18}O/^{16}O$ ratio between 25 and 75°C, e.g. Sharp et al., 2016). The kinetic fractionation exponent, θ_k, can be estimated at first order by using Graham's law (Young et al., 2002):

$$\theta_k = \ln(m_{28}/m_{29}) / \ln(m_{28}/m_{30}) \quad (8)$$

giving a value of θ_k = 0.5092, but complex kinetic fractionations in nature could have different θ_k.

With high precision triple Si isotope measurement, potential deviations from a given mass-dependent fractionation line can be observed in the $\delta'^{29}Si$-$\delta'^{30}Si$ diagram. In general, these deviations could result either from nucleosynthetic anomalies and are usually noted $\varepsilon'^{29}Si$ for Si isotope data on meteorites (e.g., Pringle et al., 2013), or from variations of θ values resulting from complex mass-dependent isotopic fractionations, as it is the case potentially for Precambrian cherts. Thus, we prefer in the following to use the notation $\Delta'^{29}Si$, as done for triple oxygen isotopes in cherts. The value of $\Delta'^{29}Si$ (or of $\varepsilon'^{29}Si$) expressed in ppm is given by:

$$\varepsilon'^{29}\mathrm{Si} \text{ or } \Delta'^{29}\mathrm{Si} = (\delta'^{29}\mathrm{Si} - 0.5178 \times \delta'^{30}\mathrm{Si}) \times 1000 \quad (9)$$

3. Materials and methods

Based on previous developments of Si isotopic analysis by MC-ICP-MS at IPGP (Paris, France) (Deng et al., 2019; Pringle et al., 2014), we improved the technique for triple Si isotopes by, specifically, reducing potential isobaric interferences on Si isotopes (*Appendix*). This technique returns $2\sigma_{SE}$ for $\Delta'^{29}Si$ between 3 to 8 ppm. This precision is sufficient to detect whether Si isotopes are fractionated by equilibrium (θ_{eq} = 0.5178) or kinetic (θ_k = 0.5092) processes in case of $\delta'^{30}Si$ variations $\geqslant$ 0.5‰ (a variation of $\Delta'^{29}Si$ by 8.6 ppm is predicted for a 1‰ fractionation of $\delta'^{30}Si$ by a kinetic process). In addition to Si isotopic compositions, $\delta'^{18}O$ compositions of the cherts that were not available from previous studies were measured by ion microprobe (MC-SIMS) at CRPG-CNRS (Nancy, France) using standard procedures previously described (Marin et al., 2010; Robert and Chaussidon, 2006). The major and minor element contents were measured by ICP-MS at IPGP after acid digestion of the same powders of samples that were used for the triple Si isotopic measurements (*Appendix*).

Cherts were collected by S.M. Awramick and the Precambrian Paleobiology Research Group (PPRG, Schopf and Klein, 1992), including one Neoproterozoic chert (Bitter Springs Fm., 0.8 Ga), eight Mesoproterozoic cherts (Jixian section, 1.35 - 1.50 Ga), two Paleoproterozoic cherts (Gunflint Fm., 2.0 Ga) and five Archean cherts (Tumbiana Fm., Onverwacht Grp., Warrawoona Grp., 2.72-3.50 Ga). These samples have been previously studied for their $\delta^{18}O$ and $\delta^{30}Si$ (Marin et al., 2010; Marin-Carbonne et al., 2012; Robert and Chaussidon, 2006) and their geological settings have been described (*Appendix*). The eight Jixian samples were chosen to study in more details the origin of possible Si isotopic variations within a given Proterozoic sedimentary basin which contains thick layers of interbedded carbonates and cherts that were sedimented after a rifting event at 1.6 Ga (Li et al., 2013).

4. Results

All the cherts, by definition, contain mostly silica, but non-siliceous veins and inclusions are frequently observed. Chert fragments devoid of veins and inclusions were carefully handpicked for analysis. However, while most cherts have bulk SiO_2 contents > 90 *wt*%, two samples (Jixian 8 of 8/18/83 and Jixian 8/18/83, Table S2) have lower SiO_2 contents due to the presence of high contents of either Al_2O_3 and K_2O (6.34 *wt*% Al_2O_3 and 8.01 *wt*% K_2O for Jixian 8 of 8/18/83). Otherwise, all cherts have low and variable contents of minor elements with no significant differences between the Jixian suite (0.03 - 1.31 *wt*% CaO, 0.05 - 0.90 *wt*% MgO, 0.01 - 1.02 *wt*% FeO), the 2.09 Ga Gunflint samples (0.05 - 1.50 *wt*% CaO, 0.06 - 0.73 *wt*% MgO, 0.88 - 1.17 *wt*% FeO, 0.09 - 0.31 *wt*% Al_2O_3, consistent with previous ion probe data in Marin-Carbonne et al., 2012), and the Archean cherts ($\leqslant$ 0.45 *wt*% CaO, $\leqslant$ 0.16 *wt*% MgO, 0.13 - 0.87 wt% FeO, 0.14 - 1.14 wt% Al_2O_3, consistent with the compositions previously reported, Hofmann et al., 2013; Sugitani, 1992; Sugitani et al., 2006). Note also that variations in Al_2O_3, TiO_2, K_2O and Zr are often positively correlated. The $\delta^{18}O$ values measured for the Jixian cherts range from 23.1‰ to 29.3‰, which is within the ranges previously found (e.g., 10.09 - 28.43‰ in (Robert and Chaussidon, 2006), 15.7-27.8‰ in (Ding et al., 2017). All the $\delta^{18}O$ values of the present cherts are consistent with the general trend of decreasing $\delta^{18}O$ values with age established by (Fig. 1A, Knauth and Lowe, 1978).

The present cherts show a large range of variations for $\delta'^{30}Si$ values from -1.139 ± 0.025‰ to 2.925 ± 0.014‰, Neoproterozoic and Mesoproterozoic cherts having more positive $\delta'^{30}Si$ values than Paleoproterozoic ones (Table 1, Fig. 1B). This range of variations and this systematics are consistent with previous *in situ* data (Robert and Chaussidon, 2006; Sengupta and Pack, 2018; Tartèse et al., 2017) and bulk data (Chakrabarti et al., 2012; Ding et al., 2017). The present data confirm the large range (~ 3‰, from 0.170 to 2.925‰) of $\delta'^{30}Si$ values for Jixian cherts, previously observed with in situ data (0.76 - 4.53‰, Robert and Chaussidon, 2006) and bulk data (0.5 - 3.9‰, Ding et al., 2017). Overall, there is a clear positive correlation between the present bulk $\delta'^{30}Si$ values and the previous ion probe $\delta^{30}Si$ data, however with some scatter (Fig. S3). This is likely due to the fact that the ion probe data were collected only in microquartz while the present bulk $\delta'^{30}Si$ data are an average of the different forms of silica in the cherts (microquartz, veins of hydrothermal quartz, detrital quartz grains) which have been shown by ion probe to have potentially different $\delta^{30}Si$ values in a given chert (Marin-Carbonne et al., 2012). The present bulk $\delta'^{30}Si$ values show a broad positive trend with the microquartz $\delta^{18}O$ values (Fig. S8), as observed previously between $\delta^{30}Si$ and $\delta^{18}O$ values on microquartz (Robert and Chaussidon, 2006), suggesting that the bulk $\delta'^{30}Si$ values are primarily controlled by the composition of the microquartz.

A significant range of $\Delta'^{29}Si$ values, from -20 ± 4 to 28 ± 4 ($2\sigma_{SE}$), is observed in the present cherts (Table 1). This could not be detected previously given the lower precision of published data (Pringle et al., 2014). In the triple Si isotopes diagram ($\delta'^{29}Si$-$\delta'^{30}Si$), the Jixian samples plot between the theoretical equilibrium and the kinetic mass-dependent fractionation lines assumed to cross at the Si isotopic composition of mantle basalts as represented by the BHVO-2 standard ($\delta^{30}Si$ = -0.31‰ and $\delta^{29}Si$ = -0.16‰, Pringle et al., 2014) and define a slope of 0.5123 ± 0.0022

187 ($2\sigma_{SE}$). In a $\Delta'^{29}Si$-$\delta'^{30}Si$ diagram this gives a slope of -5.51 ± 2.16 ($2\sigma_{SE}$) between the equilibrium and kinetic mass
188 fractionation lines (Fig. 3A). There is no clear trend of $\Delta'^{29}Si$ values with age (Fig. 1C), the most positive $\Delta'^{29}Si$ are
189 present in the 3.5 Ga cherts ($\Delta'^{29}Si$ values from 7 ± 8 to 28 ± 4 ppm) while the most negative $\Delta'^{29}Si$ values are in the
190 Jixian cherts. The 3.5 Ga cherts do not plot on the $\Delta'^{29}Si$-$\delta'^{30}Si$ line defined by the Jixian cherts (Fig. 2).

191 ## 5. Discussion

192 ### 5.1 Three-endmember sources of SiO_2 in cherts

193 The systematic variations between the chemical compositions and the $\delta'^{30}Si$ values of the present cherts
194 imply the existence of three sources for Si in cherts. The first one is detrital silica, clearly observed in cherts with high
195 Al_2O_3 contents (3.77 - 6.34 *wt*%). These cherts have $\delta'^{30}Si$ values close to 0‰, as expected for detrital particulate
196 silica from the continents which is likely to have a $\delta'^{30}Si$ close to that estimated for the bulk upper continental crust
197 (-0.25 ± 0.16‰, Savage et al., 2013). The positive trend between Al_2O_3 and K_2O contents (Fig. S5), regardless of chert
198 types and ages, points to the systematic presence in cherts of detrital materials from the continents(Marin-Carbonne
199 et al., 2012; Sugitani et al., 2002; Van den Boorn et al., 2010). Detrital silica would be characterized by high Al_2O_3
200 contents with a range of Al_2O_3/K_2O ratios reflecting the compositional range of the continental source (Sugitani et
201 al., 2002). Because of the secular increase of the volume of continental crust, the fraction of detrital silica in cherts
202 has likely increased with time, which could explain why the highest fraction of detrital silica is observed in some
203 Jixian cherts. The two other sources of silica can be clearly identified in cherts with low Al_2O_3 content (< 0.48 *wt*%)
204 which have a range of $\delta'^{30}Si$ values from 0.32 ± 0.04‰ to 2.93 ± 0.01‰ (Fig. 5A). A similar $\delta'^{30}Si$-Al_2O_3 systematics
205 was observed in 3.5 Ga cherts from the Pilbara craton (Van den Boorn et al., 2010) and interpreted as reflecting the
206 presence in these cherts of (i) chemical precipitates (named C-cherts and Al_2O_3-poor) from a mixture between
207 Archean seawater (positive $\delta'^{30}Si$ values) and hydrothermal fluids (negative $\delta'^{30}Si$ values) and of (ii) volcanic materials
208 silicified by seawater (Al_2O_3-rich and slightly positive $\delta^{30}Si$ values).
209 As also previously observed (Van den Boorn et al., 2010), the presence in cherts of silica of various origins
210 is reflected in the variations of the cherts REE contents. This is observed for the present Jixian cherts where the ones
211 with high Al_2O_3 content have the highest total REE contents (39.29 - 84.50 ppm) and are enriched in LREE similarly
212 to the upper continental crust (PAAS, Taylor and McLennan, 1981). The cherts with low Al_2O_3 content have much
213 lower total REE contents with either a small positive Eu anomaly in agreement with a hydrothermal input (Van den
214 Boorn et al., 2010) or a strongly fractionated pattern possibly related to seawater (Fig. S7, Bolhar et al., 2004).

215 ### 5.2 Signatures of kinetic and equilibrium processes in the silicon isotopic composition of cherts

216 The range in $\Delta'^{29}Si$ values found for the present Precambrian cherts, distributing in a $\Delta'^{29}Si$ versus $\delta'^{30}Si$
217 diagram between the lines for $\theta_{eq,max}$ (0.5178) and for θ_k (0.5092), is strongly suggestive of the fact that Si in cherts
218 records both kinetic and equilibrium Si isotopic fractionations. Though θ_{eq} has not yet been determined for

temperatures in the range from 0 to 75°C, it seems likely, by analogy with triple O isotopes as explained in section 2, that the effect of temperature cannot decrease θ_{eq} from 0.5178 to 0.5092. Similarly, θ_{k} might depart slightly from 0.5092 depending on the process fractionating Si, but no data exist to quantify this effect. In the following we consider that these potential variations of θ_{eq} and θ_{k} are second order relative to the present large range found for triple silicon isotopic compositions of cherts and we use as a first approach θ_{eq}= 0.5178 and the θ_{k} = 0.5092.

Several equilibrium and kinetic Si isotopic fractionations during the marine Si cycle and the complex formation of cherts can be expected.

(1) Considering, first, the direct precipitation of amorphous silica from seawater, the equilibrium fractionation factor $1000 \ln \alpha^{30}_{\mathrm{silica-fluid}}$ (= $\delta'^{30}Si_{silica}$ - $\delta'^{30}Si_{fluid}$, noted as $\Delta^{30}Si_{silica\text{-}fluid}$ in the following) seems to be too small to produce the >3‰ variations of $\delta'^{30}Si$ observed in Jixian cherts or Archean cherts. The most extreme values for equilibrium $\Delta^{30}Si_{silica\text{-}fluid}$, determined theoretically or experimentally under different conditions, range from -2.1 to 2.1‰ (*Appendix*). Therefore, making a chert with $\delta'^{30}Si$ of 3‰ from a fluid with dissolved silica having $\delta'^{30}Si$ ≈-0.3‰ (the value predicted for Archean seawater if dissolved silica derives predominantly from leaching of Si from the oceanic crust, Siever, 1992) would require either to fractionate the fluid by an extreme reservoir effect with a negative $\Delta^{30}Si_{silica\text{-}fluid}$ (for instance, the removal of ~90% of Si from the fluid with a $\Delta^{30}Si_{silica\text{-}fluid}$ of -2.1‰ would result in a fractionated fluid with $\delta'^{30}Si$ =-0.3-2.1×LN(0.1) = 4.5‰, from which precipitation of silica should take place and get a $\delta'^{30}Si$ of +2.4‰) or to have a very strong $\Delta^{30}Si_{silica\text{-}fluid}$ of >3.3‰, which seems unlikely since the most probable values for equilibrium $\Delta^{30}Si_{silica\text{-}fluid}$ during precipitation of silica ranges from 0.1 to 1.6‰ for 25~75°C and pH 6~9 (*Appendix*, note that we consider an average equiljibrium $\Delta^{30}Si_{silica\text{-}fluid}$ of +0.8‰ in the following discussion). Thus, larger Si isotopic fractionations of kinetic origin, either during the formation of cherts or in the marine cycle (i.e. changing the Si isotopic composition of seawater) are required.

(2) The large $\Delta^{30}Si_{silica\text{-}fluid}$ determined in some hydrothermal systems (e.g. from -2.40 to -5.49‰ at Cistern spring in Yellowstone national park, Chen et al., 2020, *Appendix*) shows that silica can be precipitated in such a system with a large kinetic isotopic fractionation. This apparent isotopic fractionation is consistent with values determined experimentally or theoretically (Oelze et al., 2014; Roerdink et al., 2015). Thus, by a reservoir effect, large kinetic Si isotopic fractionations could be present in Si delivered to seawater by hydrothermal fluids leaching the oceanic crust, as previously proposed to be one cause of increase of seawater $\delta^{30}Si$ in the Archean (Robert and Chaussidon, 2006). Studies of the silica-water system in the range 0 – 300°C have shown that a hydrothermal fluid ascending the crust and cooling rapidly will become supersaturated relative to solid silica species, leading to a rapid increase in the rate of silica precipitation (Rimstidt and Barnes, 1980). Assuming a kinetic $\Delta^{30}Si_{silica\text{-}fluid}$ ≈ -2.0‰ (Oelze et al., 2014) and θ_{k} = 0.5092, the Si remaining in the fluid and delivered to the oceans would be isotopically fractionated with $\delta'^{30}Si$ and $\Delta'^{29}Si$ values from 3.63 ‰ to 1.74 ‰ and from -34 to -18 ppm, respectively (Fig. 4). This will also result in the presence on (or below) the seafloor of hydrothermal silica with strongly negative $\delta'^{30}Si$ values

that can be remobilized during diagenesis for the formation of cherts. Amorphous silica precipitated from seawater could thus have a Si isotopic composition reflecting both a source effect (kinetically fractionated hydrothermal Si added to seawater) and the process of precipitation itself (at equilibrium with seawater).

(3) The growth of continents made rivers to become an important Si flux to seawater, presumably during the late Archean. Even if there was no biogenic uptake of dissolved Si in rivers by plants in the Archean (one of the major Si fractionation in soils waters today, e.g. Sun et al., 2016), it is reasonable to assume that dissolved Si in river had an isotopic composition kinetically fractionated. First, the large fractionation in hotsprings has been proven to be kinetic as discussed above. Second, the flow-through experiment by Geilert et al 2014 suggests a kinetic precipitation with $\Delta^{30}Si_{silica\text{-}fluid}$ from -2.1 to -0.5‰ at surface conditions and at temperatures of 10~40˚C. Futhermore, adsorption processes during the formation of secondary minerals are kinetic and have a $\Delta^{30}Si_{solid\text{-}fluid}$ between -1.5‰ and -3.3‰ (Oelze et al., 2015; Zheng et al., 2016). Thus, dissolved Si in late Archean rivers was probably kinetically fractionated and enriched in heavy Si isotopes.

(4) Another process which has been proposed to control seawater Si isotope composition is the formation of banded iron formations (BIF) and, in marine sediments, of authigenic clays. Modeling of the marine Si cycle in the Precambrian has shown that the observed change of chert $\delta^{30}Si$ could be explained, dominantly, by a change in the relative proportions of amorphous silica and authigenic clays formed, both phases removing Si from seawater and pore waters (Trower and Fisher, 2019). Unfortunately, there is at present no Si isotope data that allow to constrain precisely the Si isotopic fractionation that takes place during the formation of authigenic clays. In the following we use the isotopic fractionation ($\delta^{30}Si$ of authigenic clays is 2‰ lower than that of amorphous silica) taken by Trower and Fisher (2019) in their model. We consider that this fractionation is equilibrium and not kinetic, as it is the case for amorphous silica precipitation, though this is clearly a point that must be studied in the future.

5.3 Implications of triple silicon isotopes on the formation of the 1.5 Ga Jixian cherts

The silicon isotopic variations ($\delta'^{30}Si$ and $\Delta'^{29}Si$) observed in the suite of Jixian cherts can be understood as reflecting the presence of different silica components formed with different isotopic fractionation factors (Fig. 3C, 3D). In the following working model (Fig. 3), we try to explore, first, how the different major sources and sinks of marine Si will control the Si isotope composition of amorphous silica in a $\Delta'^{29}Si$ versus $\delta'^{30}Si$ space, and then, how the formation of cherts will modify the Si isotopic composition in this space.

We consider that during the Proterozoic, dissolved Si in seawater was (i) recharged by rivers and hydrothermal fluids leaching the oceanic crust and (ii) extracted by the precipitation of amorphous silica and the formation of authigenic clays. Assuming a temperature of seawater at 1.5 Ga ≈ 40°C (Marin et al., 2010) and hydrothermal fluids initially at 300°C at depth in the oceanic crust, 85% of dissolved silica in the hydrothermal fluids would kinetically precipitate as hydrothermal quarz with average $\delta'^{30}Si$ and $\Delta'^{29}Si$ of -1.23‰ and 8 ppm, respectively.

Slightly warmer or cooler oceans would not modify the general relationship predicted between $\delta'^{30}Si$ and $\Delta'^{29}Si$ in Fig. 3D and Fig. 4. Si remaining in the hydrothermal fluids is fractionated to $\delta'^{30}Si$ = 2.47‰ and $\Delta'^{29}Si$ = -24 ppm (Fig. 4), and mixed with dissolved Si from rivers. The flux and $\delta'^{30}Si$ of rivers in Precambrian is not well constrained but the Si isotopic composition can be assumed to be $\delta'^{30}Si \approx 1$‰ (slightly lower than modern rivers due to the absence of biogenic uptake of Si) and with a kinetic isotopic signature (see previous section) so that $\Delta'^{29}Si \approx -11$ ppm. Depending on the relative fluxes of hydrothermal Si and riverine Si, seawater would have a Si isotopic composition in between these two endmembers (see Fig. 3D). Assuming a relative flux of Si uptake from seawater by formation of authigenic clays and amorphous silica of 60% and 40%, respectively (Trower and Fischer, 2019) and isotopic fractionations described in previous section, by mass balance, the seawater $\delta'^{30}Si$ would be increased by 0.4‰ without change in $\Delta'^{29}Si$ (Fig. 3D). Amorphous silica precipitated from seawater is thus expected to have a range in Si isotopic composition with $\delta'^{30}Si$ from 1.8 to 3.7 ‰ and $\Delta'^{29}Si$ from -11 to -24 ppm (Fig. 3D).

Upon diagenesis, chert is formed with Si coming from amorphous silica, hydrothermal quartz and detrital quartz. Because the Si isotopic composition of detrital silica from the continents ($\delta'^{30}Si$ = -0.25 ± 0.16 ‰ and $\Delta'^{29}Si$ assumed to be 0 ppm) plots in Fig. 3D nearly on the mixing line between hydrothermal silica and amorphous silica, the presence of various proportions of these three components in the precursors of Jixian cherts results in the negative linear trend observed for Jixian cherts (Fig. 3D), which is between theoretical equilibrium and kinetic isotopic fractionation lines. Taking Al_2O_3 content as a proxy for the detrital input from the continents, the clear systematics observed for Precambrian cherts between $\Delta'^{29}Si$ values and Al_2O_3 contents (Fig. 5B) is consistent with inferences made in section 5.1 from the systematics between $\delta'^{30}Si$ values and Al_2O_3 contents. It can be explained by a mixture among three types of silica: (i) a detrital end-member with high Al_2O_3 contents and with $\delta'^{30}Si$ and $\Delta'^{29}Si$ close to -0.25 ‰ and 0 ppm (not significantly fractionated relative to silicate Earth), (ii) amorphous silica precipitated from seawater with low Al_2O_3 and fractionated Si isotope composition (positive $\delta'^{30}Si$ and negative $\Delta'^{29}Si$), and (iii) hydrothermal silica with low Al_2O_3 and Si isotopic composition fractionated at the opposite than amorphous silica (negative $\delta'^{30}Si$ and positive $\Delta'^{29}Si$). From their Al_2O_3 contents and $\delta'^{30}Si$, we calculate that Jixian cherts contain from 27 to 89% (59% on average) of amorphous silica precursor, from 11 to 63% of hydrothermal silica precursor (36% on average), and from 0.2 to 25% of detrital silica from the continents. At variance, note that most of the present > 2.0 Ga cherts have compositions closer to the hydrothermal end-member (62% on average, Fig. 5, Table S4), even taking into account that Archean oceans might have been warmer than 40°C (see table S3).

5.4 Triple Si isotopes evidences for diagenetic and metamorphic secondary processes in Archean cherts

Triple Si isotopes appear key to test the presence of secondary isotopic fractionations (of O and Si) that must be taken into account for reconstruction of seawater temperature. For instance, in a $\Delta'^{29}Si$-$\delta'^{30}Si$ diagram, some Archean cherts plot outside the field defined by the equilibrium and kinetic fractionation lines ($\Delta'^{29}Si$ > 10 ppm at $\delta^{30}Si$ around ~ 0‰, Fig. 2). Such isotopic compositions cannot be produced by mixing hydrothermal and seawater amorphous silica precursors fractionated from a fluid leaching the oceanic crust, even considering there was less or

no river flux (Fig. 3A, 3B) and whatever the temperatures considered for seawater. Note that the addition of continental detrital Si does not move the Si isotopic composition of chert outside this field. Thus, the presence of positive $\Delta'^{29}Si$ for a $\delta'^{30}Si$ close to 0‰ (as in most of the present Warrawoona and Onverwacht cherts) requires the occurrence of processes resulting in additional Si isotopic fractionations. These processes remain yet unclear but the fact that the highest $\Delta'^{29}Si$ are associated to the lowest $\delta'^{18}O$ values (from 13.6 to 15.4‰, Table 1, Fig. 2) indicates the possibility of strong effects of diagenesis and metamorphism (Marin et al., 2010). An appropriate combination of kinetic and equilibrium isotopic fractionations (1/3×kinetic+2/3×equilibrium, Roerdink et al., 2015) during dissolution and reprecipitation of SiO_2 at 150°C would for instance result in a slope of -0.43 in the $\Delta'^{29}Si$-$\delta'^{30}Si$ diagram (Fig. S6). This would allow to move the initial Si isotopic composition of a chert to the composition observed in some of the present > 2.0 Ga cherts during several successive steps of dissolution/re-precipitation of silica. In such a scenario, the original silica would have had a Si isotopic composition of $\delta'^{30}Si$ ~ 0.76 ‰ and $\Delta'^{29}Si$ ~ -5 ppm, such an isotopic composition necessitating a seawater temperature at around 60˚C (Fig. 3A, 3B). At variance, the five fragments of the Tumbiana chert studied plot close to the hydrothermal end-member in the $\Delta'^{29}Si$-$\delta'^{30}Si$ diagram (Fig. 2), in agreement with previous inferences made from $\delta'^{30}Si$ values and concentrations of Al_2O_3, K_2O, TiO_2 and FeO (Marin-Carbonne et al., 2012). Thus, a possible criterion to select Precambrian cherts for seawater temperature reconstruction, in addition to the criteria described in (Marin-Carbonne et al., 2014), is that their Si isotopic compositions remain between the equilibrium and kinetic lines in the $\Delta'^{29}Si$-$\delta'^{30}Si$ diagram. In such samples (e.g., present Tumbiana and Gunflint samples), microquartz with high $\delta^{18}O$ is likely deriving from silica precipitated from seawater.

5.5 Potential consequences for triple oxygen isotope systematic

The identification of kinetic isotopic fractionations for Si in cherts from their $\Delta'^{29}Si$-$\delta'^{30}Si$ systematics has potential consequences on the use of triple oxygen isotope compositions to reconstruct paleotemperatures. In the $\Delta'^{17}O$-$\delta'^{18}O$ diagram, many Precambrian cherts have triple oxygen isotopic compositions plotting to the left of the curve calculated for equilibrium with ice-free seawater (Fig 6, Sharp et al., 2016). This shift can be explained by a lower $\delta'^{18}O$ for the Archean Ocean (Sengupta et al., 2020), the involvement of meteoric waters or hydrothermal fluids during the formation of cherts, or secondary processes such as alteration and metamorphism (Abraham et al., 2011; Knauth and Epstein, 1976; Marin et al., 2010; Marin-Carbonne et al., 2012). In addition, the diagenetic transformations of opal-A to opal-CT and to microquartz can also lead to deviations from the equilibrium curve with seawater (Ibarra et al., 2022). A recent study observed the consistency of triple O isotopes between modern altered oceanic crust and Archean altered eclogite, thus precluding an Archean Ocean having a different O isotopic composition from modern seawater (McGunnigle et al., 2022) and suggesting a stronger hydrothermal alteration in the Archean. However, as shown by the present triple Si isotopes data, cherts can contain a significant fraction of silica isotopically fractionated by kinetic processes, which was not considered in previous triple O isotopes studies. This fraction of the chert would have a triple oxygen isotopic composition plotting far to the left of the equilibrium

curve with seawater in the $\Delta'^{17}O$-$\delta'^{18}O$ diagram (Fig. 6). It is not clear whether the kinetic signature of O isotopes in silica can be erased by exchange with pore water or diagenetic fluid, while that of Si would be preserved. This might be possible because of the low solubility of silica in water (water-rock interaction at 60˚C would dissolve 215 ppm SiO_2), the O_{fluid}/O_{rock} ratio ($\approx 2.7\times10^4$) is 4 orders of magnitude higher than Si_{fluid}/Si_{rock} (≈ 2.4). Nevertheless, it suggests that bulk triple O isotopic measurements of cherts to reconstruct paleotemperatures should systematically be associated to triple Si isotopic measurements to check for the presence of silica isotopically fractionated by kinetic processes.

6. Conclusion

New high precision measurements of triple silicon isotopes in Precambrian cherts allow to identify small deviations between pure equilibrium and pure kinetic mass-dependent isotopic fractionations. The chemical contents, oxygen isotopes and the triple silicon isotopes in Jixian cherts imply that these cherts are made from components having three sources: detrital quartz from the continents, hydrothermal quartz kinetically precipitated from hydrothermal fluids close to the interface between seawater and the oceanic crust, and amorphous silica precipitated at equilibrium from seawater. Archean cherts have Si isotopic compositions suggestive of successive dissolution and reprecipitation of silica during diagenesis by both kinetic and equilibrium processes. This might cause a bias when these samples are used for paleo-seawater temperature reconstructions from triple O isotopes, depending on the extent to which the precursors of cherts had their O isotopic composition fractionated by kinetic processes and on whether they were re-equilibrated with seawater during diagenesis. In any case, triple silicon isotope data represent a useful additional criteria to select Precambrian cherts for paleotemperature reconstructions. Finally, the present triple Si isotopic data are consistent with high temperatures for Archean oceans, but a more precise statement would require further work to (i) calibration of the effect of temperature on β_{eq} for $\alpha_{\mathrm{silica-water}}$ and (ii) better determination of the triple Si isotopic fractionations for the other processes which participate to the control of the Si isotopic composition of seawater, namely riverine inputs and authigenic clays formation.

CRediT authorship contribution statement

Haoxuan Sun: methodology, analyses, interpretation, writing. **Marc Chaussidon:** design of the project, interpretation, writing and funding. **François Robert:** interpretation, writing. **Shengyu Tian:** methodology. **Zhengbin Deng:** methodology. **Frédéric Moynier:** interpretation, writing and funding.

Declaration of competing interest

The authors declare that they have no known competing financial interests or personal relationships that could have appeared to influence the work reported here.

Acknowledgements

This work was supported by IPGP multidisciplinary program PARI, by Paris–IdF region SESAME Grant no. 12015908, and by INSU-CNRS PNP grant 2022.

Appendix. Supplementary material

Supplementary material related to this article can be found below.

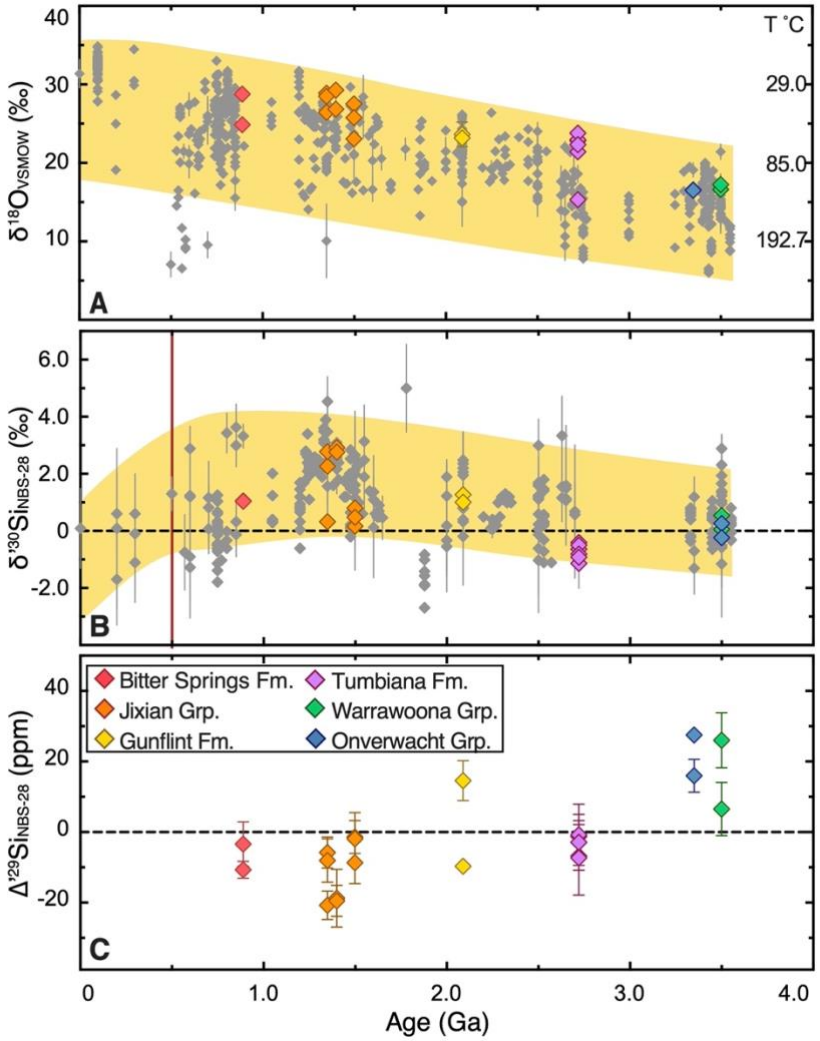

388 **Figure 1.** Oxygen and silicon isotopic compositions of Precambrian cherts versus age, $\delta^{18}O$ of microquartz in A, $\delta^{30}Si$
389 in B and $\Delta'^{29}Si$ in C. Data from this study (colored, Table 1) and from literature (in grey, Abraham et al., 2011;
390 Chakrabarti et al., 2012; Ding et al., 2017; Hren et al., 2009; Knauth, 2005; Knauth and Epstein, 1976; Knauth and
391 Lowe, 1978; Liljestrand et al., 2020; Marin et al., 2010; Marin-Carbonne et al., 2012; Robert and Chaussidon, 2006)
392 are plotted with their two standard error ($2\sigma_{SE}$). Both $\delta^{18}O$ and $\delta^{30}Si$ values show large variations at a given age. The
393 $\delta^{18}O$ and $\delta^{30}Si$ values of the cherts in this report are consistent with literature data. Precambrian cherts show
394 significant variations of their $\Delta'^{29}Si$, with a tendency for higher $\Delta'^{29}Si$ for the oldest cherts. The yellow colored field
395 are qualitative.

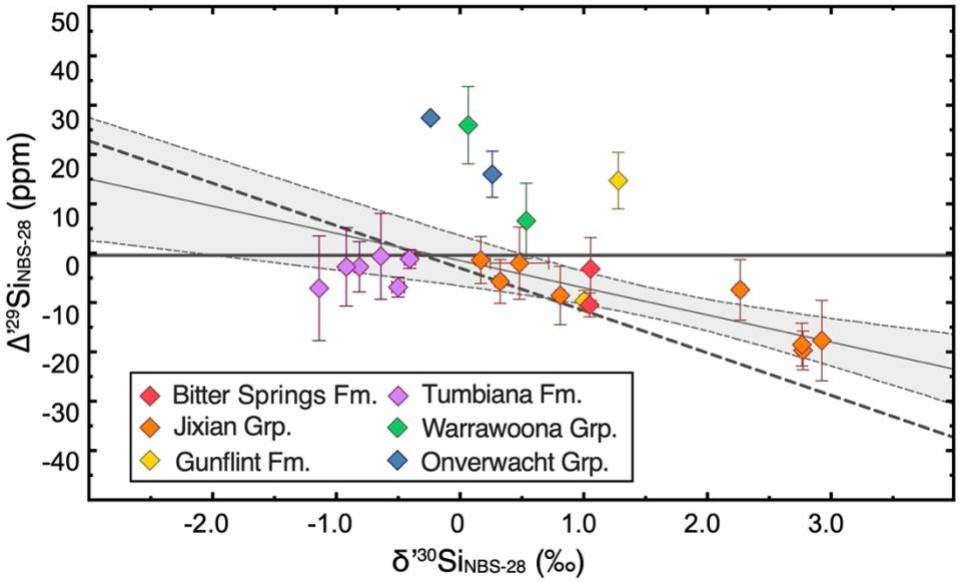

396 **Figure 2.** Details of triple silicon isotopic variations ($2\sigma_{SE}$) in cherts. The theoretical line (dashed black) for kinetic
397 isotopic fractionation (slope -8.6) is considered to intersect the horizontal equilibrium isotopic fractionation line
398 (solid black) at $\delta^{30}Si$ = -0.3‰ (i.e. the value for bulk silicate Earth). The linear regression through Jixian cherts gives a
399 slope of -5.51 ± 2.16 and a horizontal intercept of -0.262 ± 0.967 ($2\sigma_{SE}$), which correspond to a slope of 0.5123 ±
400 0.0022 ($2\sigma_{SE}$) in $\delta'^{29}Si$-$\delta'^{30}Si$ diagram (the grey zone representing the 95% confidence interval of the fit). The Jixian
401 line is in between the theoretical equilibrium and kinetic isotopic fractionation lines.

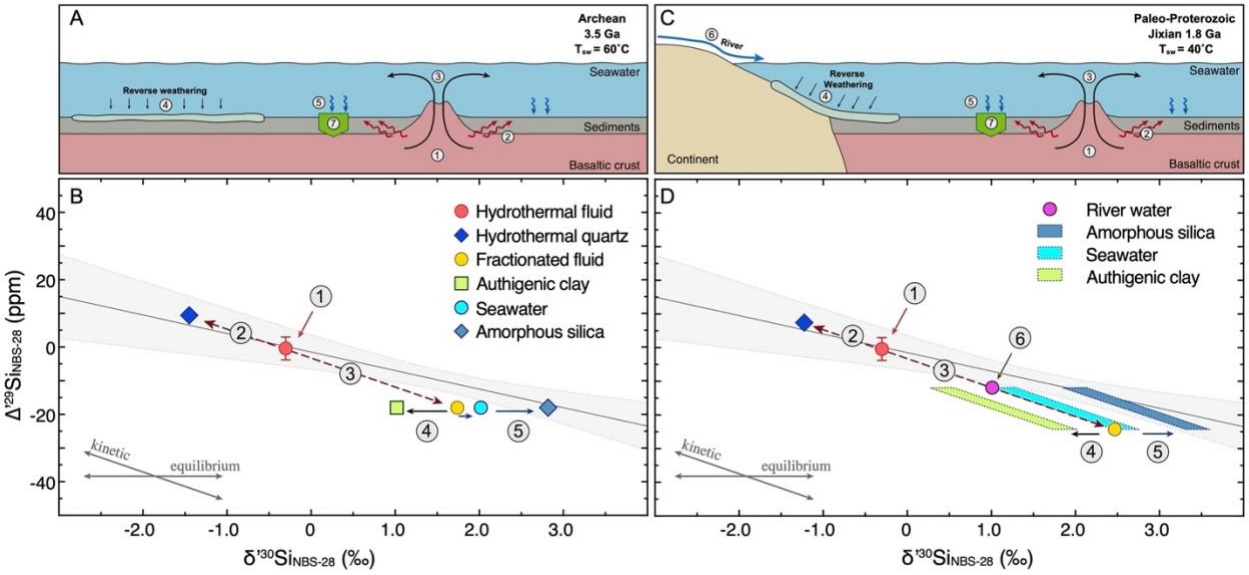

Figure 3 Models for the origin of the triple silicon isotopic variations in early Archean cherts (A&B, seawater temperature at 60˚C) and the Jixian cherts (C&D, seawater temperature at 40˚C). ① Hydrothermal leaching of Si from the oceanic basaltic crust ($\delta'^{30}Si$ = -0.30 ± 0.02 ‰) takes place with no Si isotopic fractionation. The kinetic Si isotopic fractionation during the precipitation of hydrothermal quartz (assuming $\Delta^{30}Si_{quartz\text{-}fluid}$ = -2.0‰ and following a trajectory with a slope of -8.6) will ② deplete ^{30}Si in hydrothermal quartz relative to hydrothermal fluids and by mass balance will ③ release into seawater a strongly kinetically fractionated fluid enriched in ^{30}Si. ④ Reverse weathering and ⑤ precipitation of amorphous silica take place to maintain dissolved Si saturated in seawater. Si isotopic fractionations for both processes are expected to be at equilibrium ($\Delta^{30}Si_{chert\text{-}sw}$ = +0.8‰ see *Appendix*, and $\Delta^{30}Si_{clay\text{-}chert}$ = -2‰, Trower and Fisher, 2018). Considering that the uptake of dissolved Si by reverse weathering can represent up to 60% of the total Si uptake, $\delta'^{30}Si_{sw}$ will increase by ≈0.4‰. Since the late Archean, the growth of continents made that ⑥ rivers became another important Si flux to seawater. The blue field in D represents the possible Si isotopic composition of seawater in Jixian times (assuming kinetic Si isotopic fractionation during continental weathering and average $\delta'^{30}Si_{river}$ = 1‰, see refs in text). ⑦ Formation of chert.

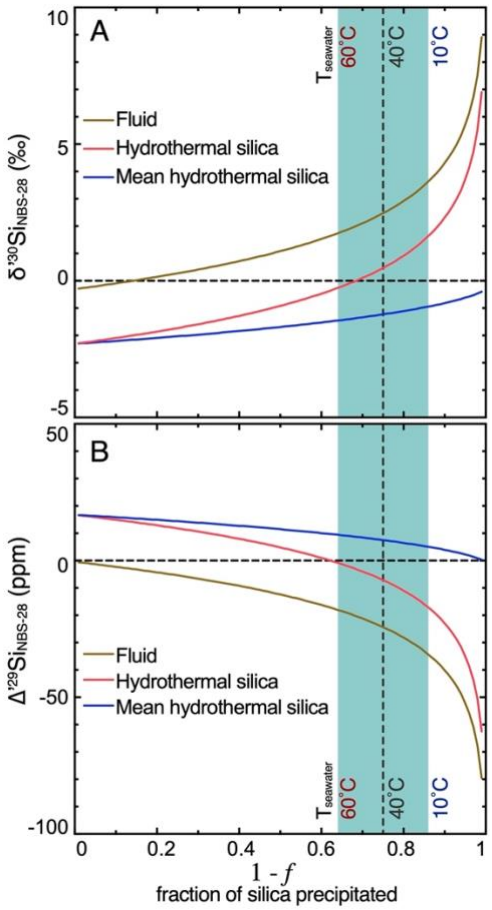

Figure 4. Fractionation of Si isotopes during precipitation of hydrothermal quartz due to cooling of hydrothermal fluids ascending in the oceanic crust (panel A for $\delta^{30}Si$, panel B for $\Delta'^{29}Si$). The Si isotopic composition of the fluid is given by the Rayleigh equation $\delta^{30}Si_{fluid} = \delta^{30}Si_{initial} + \Delta^{30}Si_{solid\text{-}fluid} \times \ln(f)$, with f the fraction of Si remaining in the fluid at the temperature of seawater (*f* being the ratio of the solubility of amorphous silica at the temperature of seawater to the solubility of hydrothermal quartz at the temperature of the initial fluid, Robert and Chaussidon (Robert and Chaussidon, 2006). The initial hydrothermal fluid is assumed to have a temperature of 300˚C and the Si isotopic composition of fresh oceanic crust (i.e., the same than BHVO-2, $\delta^{30}Si$ = -0.3‰ and $\Delta'^{29}Si$ = 0). The value of *f* ranges from 0.14 to 0.36 (blue field in Fig S8) for a seawater temperature ranging from 10 to 60°C. Taking a value of $\Delta^{30}Si_{solid\text{-}fluid}$ of -2.00‰ (Chen et al., 2020) and a θ value characteristic of a kinetic process (0.5092), this gives a range for $\delta^{30}Si$ and $\Delta'^{29}Si$ values of hydrothermal silica from -0.94‰ to -1.45‰ and from 0.05 to 0.10, respectively. Consequently, dissolved Si delivered to the oceans will have $\delta^{30}Si$ and $\Delta'^{29}Si$ values from 3.63‰ to 1.74‰ and from -34 to -18, respectively.

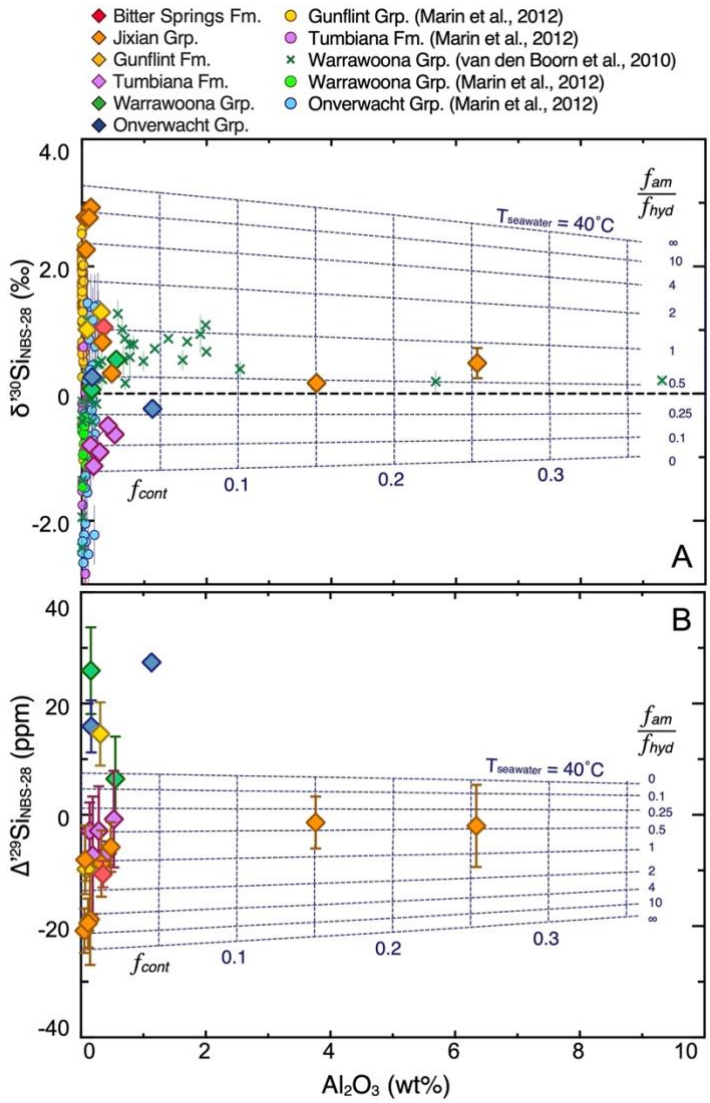

Figure 5. Constraints from Si isotopic compositions and Al_2O_3 contents on the fraction of the three possible sources of silica in the precursors of Precambrian cherts [present data and data from (Marin-Carbonne et al., 2012; Van den Boorn et al., 2010)]: detrital continental silica (f_{cont} shown as vertical dashed lines calculated for a continental end member with 60% silica and 25% Al_2O_3), amorphous silica considered to have precipitated from seawater at 40˚C (f_{am}), and hydrothermal silica (f_{hyd}). The horizontal dashed lines show the ratio f_{am}/f_{hyd}. Note the large variations among Precambrian cherts in the f_{am}/f_{hyd} ratios. Note also that most of the present Archean cherts have $\Delta'^{29}Si$ that cannot be explained by this mixing model and require additional Si isotopic fractionations.

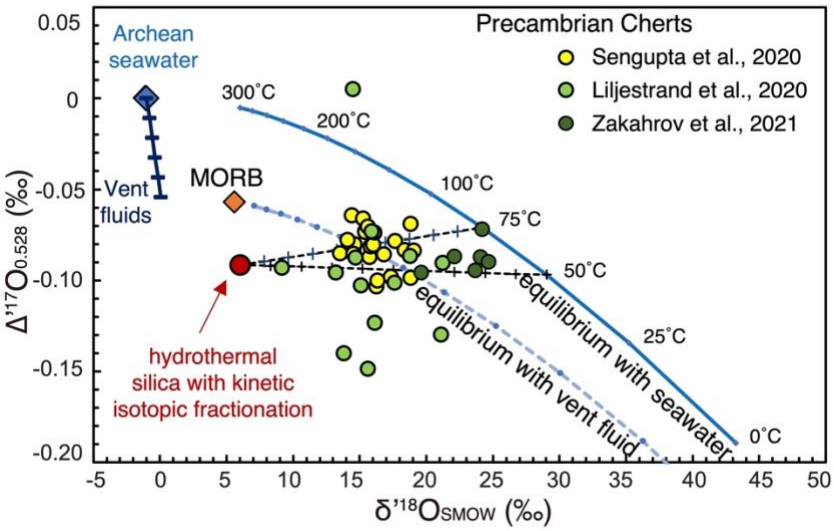

434 **Figure 6.** Possible effects of the presence of oxygen kinetic isotopic fractionations on the triple oxygen isotopes
435 systematics of Archean cherts. The linearized delta notation is used with $\delta'^{xx}O=1000\times\ln(\delta^{xx}O/1000+1)$, where ^{xx}O
436 represents ^{17}O and ^{18}O, and $\Delta'^{17}O=\delta'^{17}O-0.528\times\delta'^{18}O$. To keep the diagram simple, we have chosen 3 representative
437 sets of data for Precambrian cherts from (Liljestrand et al., 2020; Sengupta et al., 2020; Zakharov et al., 2021). Mid
438 Ocean Ridge Basalt (MORB) representing unaltered oceanic crust is from (Pack and Herwartz, 2014; Sharp et al.,
439 2016). Vent fluids corresponding to a mixture between seawater and hydrothermal fluids at equilibrium with MORB
440 are shown following the approach of (Zakharov et al., 2021). The red dot is for a possible oxygen isotopic composition
441 of hydrothermal silica fractionated by a kinetic isotopic fractionation (using 0.515 instead of 0.528 for the
442 relationship between $\delta'^{17}O$ and $\delta'^{18}O$). The presence in various proportions of such hydrothermal silica in a chert
443 with microquartz formed at equilibrium with seawater between 50 and 75°C (mixing relationships shown as dashed
444 black lines) could explain part of the range observed for the triple oxygen isotopic compositions of Precambrian
445 cherts.

Sample	Age (Ga)		MC-ICP-MS										SIMS bulk					
			$\delta'^{29}Si$	2sd	2se	**$\delta'^{30}Si$**	2sd	2se	**$\Delta'^{29}Si$**	2sd	2se	n	$\delta'^{18}O$	2se		n	$\delta'^{30}Si$	se	
Bitter Springs Fm.																			
BitterSprings 5 of 5/11/90	0.89	a	**0.544**	0.012	0.004	**1.057**	0.023	0.008	**-3**	18	6	8	24.9	0.8	a		3.33	0.21	a
BitterSprings 5 of 5/11/90_rp			**0.532**	0.040	0.016	**1.047**	0.069	0.028	**-10**	6	2	6	28.8	0.3		10			
BitterSprings 5 of 5/11/90 Average	0.89	a	***0.538***	*0.018*	*0.012*	***1.052***	*0.014*	*0.010*	***-7***	*10*	*7*	*2*							
Jixian																			
Jixian 2A of 8/18/83	1.35	a	**0.162**	0.059	0.021	**0.324**	0.111	0.039	**-6**	13	5	8	26.45	0.33		10			
Jixian 2b of 8-16-83	1.35	a	**1.166**	0.051	0.025	**2.267**	0.076	0.038	**-7**	12	6	4	28.92	0.12		10	3.48	0.55	a
Jixian 3b of 8-16-83	1.35	a	**1.416**	0.038	0.011	**2.772**	0.072	0.021	**-20**	14	4	12	28.49	0.37		10	2.45	0.79	a
Jixian 5a of 8/12/93	1.40	a	**1.497**	0.028	0.014	**2.925**	0.029	0.014	**-18**	16	8	4	26.84	0.17		10			
Jixian 5b of 8/12/93	1.40	a	**1.414**	0.052	0.015	**2.766**	0.092	0.027	**-18**	15	4	12	29.32	0.20		10			
Jixian 2 of 8/18/83	1.50	a	**0.412**	0.094	0.021	**0.812**	0.169	0.038	**-9**	27	6	20	27.52	0.17		10	2.14	0.31	a
Jixian 8/18/83	1.50	a	**0.087**	0.082	0.024	**0.170**	0.158	0.045	**-1**	16	5	12	25.82	0.98		9			
Jixian 8 of 8/18/83	1.50	a	**0.248**	0.329	0.116	**0.483**	0.665	0.235	**-2**	21	7	8	23.09	0.64		6	1.16	0.29	a
Gunflint Fm.																			
Gunflint PPGR134	2.09	a	**0.678**	0.011	0.005	**1.280**	0.026	0.013	**15**	11	6	4	23.6	1.6	a		0.83	0.55	a
Gunflint 3 of 6/30/84			**0.500**	0.018	0.009	**0.986**	0.039	0.020	**-11**	15	7	4							
			0.524	0.043	0.025	**1.029**	0.085	0.049	**-9**	7	4	3							
Gunflint 3 of 6/30/84 Average	2.09	a	***0.512***	*0.035*	*0.024*	***1.008***	*0.061*	*0.043*	***-10***	*3*	*2*	*2*	23.3	1.0	b		0.8	0.6	b
Tumbiana																			
Tumbiana 1 of 07/06/90			**-0.222**	0.029	0.008	**-0.427**	0.045	0.013	**0**	14	4	12							
			-0.200	0.018	0.011	**-0.383**	0.022	0.012	**-2**	13	7	3							
Tumbiana 1 of 07/06/90 Average	2.72	b	***-0.211***	*0.030*	*0.021*	***-0.405***	*0.063*	*0.044*	***-1***	*3*	*2*	*2*	18.6	1.1	b		-1.10	0.90	a
Tumbiana 1 of 07/06/90_P1			**-0.331**	0.033	0.013	**-0.637**	0.029	0.012	**-1**	21	9	6	15.33	0.62		10			
Tumbiana 1 of 07/06/90_P2			**-0.266**	0.068	0.028	**-0.501**	0.123	0.050	**-7**	5	2	6	22.88	0.45		7			
Tumbiana 1 of 07/06/90_P3			**-0.422**	0.037	0.012	**-0.810**	0.067	0.022	**-3**	15	5	9	22.97	0.34		7			
Tumbiana 1 of 07/06/90_P4			**-0.597**	0.029	0.012	**-1.139**	0.060	0.025	**-7**	26	11	6	23.81	0.68		8			
Tumbiana 1 of 07/06/90_P5			**-0.477**	0.038	0.015	**-0.916**	0.067	0.027	**-3**	20	8	6	22.34	0.56		10			
Onverwacht Grp.																			
Onverwacht PPRG198	3.35	b	**0.151**	0.054	0.019	**0.261**	0.084	0.030	**16**	13	5	8	16.7	0.7	b		-0.20	0.70	b
Onverwacht 2 of 16/09/65	3.35	b	**-0.093**	0.098	0.020	**-0.234**	0.188	0.038	**28**	19	4	24							
			-0.098	0.016	0.009	**-0.241**	0.016	0.010	**27**	10	6	3							
Onverwacht 2 of 16/09/65 Average			**-0.095**	0.006	0.004	**-0.237**	0.010	0.007	**27**	1	1	2	14.8	0.5	b		-1.30	0.90	b
Warrawoona Grp.																			
Warrawoona PPRG006	3.50	a	**0.284**	0.021	0.010	**0.536**	0.043	0.022	**7**	15	8	4	14.3	0.5	b		-0.20	0.70	b
Warrawoona PPRG013	3.50	a	**0.061**	0.023	0.012	**0.069**	0.020	0.010	**26**	16	8	4	13.6	1.7	a		1.40	0.32	a
Terrestrial tandard																			
BHVO-2			**-0.156**	0.058	0.009	**-0.301**	0.107	0.016	**0**	23	3	43							
BCR-2			**-0.109**	0.075	0.037	**-0.206**	0.144	0.072	**-2**	11	5	4							
BIR-1a			**-0.124**	0.126	0.063	**-0.233**	0.217	0.108	**-4**	15	8	4							
GSP-2			**-0.121**	0.140	0.070	**-0.238**	0.232	0.116	**2**	22	11	4							
AGV-2			**-0.101**	0.071	0.035	**-0.178**	0.143	0.071	**-9**	14	7	4							

446 **Table 1.** Bulk silicon and oxygen isotopic composition of cherts and terrestrial rock standards. Data from [a]Robert and Chaissidon, 2006 and [b]Marin-Carbonne et al., 2012

Reference

Abraham, K., Hofmann, A., Foley, S., Cardinal, D., Harris, C., Barth, M., André, L., 2011. Coupled silicon–oxygen isotope fractionation traces Archaean silicification. Earth Planet Sci Lett 301, 222-230.

Audi, G., Wapstra, A., 1993. The 1993 atomic mass evaluation:(I) Atomic mass table. Nuclear Physics A 565, 1-65.

Bigeleisen, J., Mayer, M.G., 1947. Calculation of equilibrium constants for isotopic exchange reactions. J Chem Phys 15, 261-267.

Bolhar, R., Kamber, B.S., Moorbath, S., Fedo, C.M., Whitehouse, M.J., 2004. Characterisation of early Archaean chemical sediments by trace element signatures. Earth Planet Sci Lett 222, 43-60.

Chakrabarti, R., Knoll, A.H., Jacobsen, S.B., Fischer, W.W., 2012. Si isotope variability in Proterozoic cherts. Geochim Cosmochim Acta 91, 187-201.

Chen, X.-Y., Chafetz, H.S., Lapen, T.J., 2020. Silicon isotope variations in hydrothermal systems at Yellowstone National Park, Wyoming, USA. Geochim Cosmochim Acta 283, 184-200.

De La Rocha, C., Brzezinski, M.A., DeNiro, M.J., 1997. Fractionation of silicon isotopes by marine diatoms during biogenic silica formation. Geochim Cosmochim Acta 61, 5051-5056.

De La Rocha, C., Brzezinski, M.A., DeNiro, M.J., 2000. A first look at the distribution of the stable isotopes of silicon in natural waters. Geochim Cosmochim Acta 64, 2467-2477.

Deng, Z., Chaussidon, M., Guitreau, M., Puchtel, I.S., Dauphas, N., Moynier, F., 2019. An oceanic subduction origin for Archaean granitoids revealed by silicon isotopes. Nat Geosci 12, 774-778.

Ding, T., Gao, J., Tian, S., Fan, C., Zhao, Y., Wan, D., Zhou, J., 2017. The δ30Si peak value discovered in middle Proterozoic chert and its implication for environmental variations in the ancient ocean. Sci Rep 7, 1-15.

Ding, T., Wan, D., Wang, C., Zhang, F., 2004. Silicon isotope compositions of dissolved silicon and suspended matter in the Yangtze River, China. Geochim Cosmochim Acta 68, 205-216

Gaspard, F., Opfergelt, S., Dessert, C., Robert, V., Ameijeiras-Mariño, Y., Delmelle, P., 2021. Imprint of chemical weathering and hydrothermalism on the Ge/Si ratio and Si isotope composition of rivers in a volcanic tropical island, Basse-Terre, Guadeloupe (French West Indies). Chem Geol 577, 120283.

Georg, R., Reynolds, B.C., Frank, M., Halliday, A.N., 2006. Mechanisms controlling the silicon isotopic compositions of river waters. Earth Planet Sci Lett 249, 290-306.

Gregory, R., 2003. Ophiolites and global geochemical cycles: Implications for the isotopic evolution of seawater. Geological Society, London, Special Publications 218, 353-368.

Herwartz, D., 2021. Triple oxygen isotope variations in Earth's crust. Rev Mineral Geochem 86, 291-322.

Herwartz, D., Pack, A., Krylov, D., Xiao, Y., Muehlenbachs, K., Sengupta, S., Di Rocco, T., 2015. Revealing the climate of snowball Earth from Δ17O systematics of hydrothermal rocks. Proc Natl Acad Sci U S A 112, 5337-5341.

Hofmann, A., Bolhar, R., Orberger, B., Foucher, F., 2013. Cherts of the Barberton Greenstone Belt, South Africa: Petrology and trace-element geochemistry of 3.5 to 3.3 Ga old silicified volcaniclastic sediments. South Afr J Geol 116, 297-322.

Hren, M., Tice, M., Chamberlain, C., 2009. Oxygen and hydrogen isotope evidence for a temperate climate 3.42 billion years ago. Nature 462, 205-208.

Hulston, J., Thode, H., 1965. Variations in the S33, S34, and S36 contents of meteorites and their relation to chemical and nuclear effects. J Geophys Res 70, 3475-3484.

Ibarra, D.E., Yanchilina, A.G., Lloyd, M.K., Methner, K.A., Chamberlain, C.P., Yam, R., Shemesh, A., Stolper, D.A., 2022. Triple oxygen isotope systematics of diagenetic recrystallization of diatom opal-A to opal-CT to microquartz in deep sea sediments. Geochim Cosmochim Acta 320, 304-323.

Jaffrés, J.B., Shields, G.A., Wallmann, K., 2007. The oxygen isotope evolution of seawater: A critical review of a long-standing controversy and an improved geological water cycle model for the past 3.4 billion years. Earth Sci Rev 83, 83-122.

Knauth, L.P., 2005. Temperature and salinity history of the Precambrian ocean: implications for the course of microbial evolution. Palaeogeogr Palaeoclimatol Palaeoecol 219, 53-69.

Knauth, L.P., 2018. Petrogenesis of chert, Silica, pp. 233-258.

Knauth, L.P., Epstein, S., 1976. Hydrogen and oxygen isotope ratios in nodular and bedded cherts. Geochim Cosmochim Acta 40, 1095-1108.

Knauth, L.P., Lowe, D.R., 1978. Oxygen isotope geochemistry of cherts from the Onverwacht Group (3.4 billion years), Transvaal, South Africa, with implications for secular variations in the isotopic composition of cherts. Earth Planet Sci Lett 41, 209-222.

Li, H., Lu, S., Su, W., Xiang, Z., Zhou, H., Zhang, Y., 2013. Recent advances in the study of the Mesoproterozoic geochronology in the North China Craton. J Asian Earth Sci 72, 216-227.

Liljestrand, F.L., Knoll, A.H., Tosca, N.J., Cohen, P.A., Macdonald, F.A., Peng, Y., Johnston, D.T., 2020. The triple oxygen isotope composition of Precambrian chert. Earth Planet Sci Lett 537, 116167.

Lowe, D.R., Ibarra, D.E., Drabon, N., Chamberlain, C.P., 2020. Constraints on surface temperature 3.4 billion years ago based on triple oxygen isotopes of cherts from the Barberton Greenstone Belt, South Africa, and the problem of sample selection. Am J Sci 320, 790-814

Marin, J., Chaussidon, M., Robert, F., 2010. Microscale oxygen isotope variations in 1.9 Ga Gunflint cherts: assessments of diagenesis effects and implications for oceanic paleotemperature reconstructions. Geochim Cosmochim Acta 74, 116-130.

Marin-Carbonne, J., Chaussidon, M., Robert, F., 2012. Micrometer-scale chemical and isotopic criteria (O and Si) on the origin and history of Precambrian cherts: implications for paleo-temperature reconstructions. Geochim Cosmochim Acta 92, 129-147.

Marin-Carbonne, J., Robert, F., Chaussidon, M., 2014. The silicon and oxygen isotope compositions of Precambrian cherts: A record of oceanic paleo-temperatures? Precambrian Res 247, 223-234.

McGunnigle, J., Cano, E., Sharp, Z., Muehlenbachs, K., Cole, D., Hardman, M., Stachel, T., Pearson, D., 2022. Triple oxygen isotope evidence for a hot Archean ocean. Geology.

Miller, M.F., 2002. Isotopic fractionation and the quantification of 17O anomalies in the oxygen three-isotope system: an appraisal and geochemical significance. Geochim Cosmochim Acta 66, 1881-1889

Muehlenbachs, K., Clayton, R., 1976. Oxygen isotope composition of the oceanic crust and its bearing on seawater. J Geophys Res 81, 4365-4369

Oelze, M., von Blanckenburg, F., Bouchez, J., Hoellen, D., Dietzel, M., 2015. The effect of Al on Si isotope fractionation investigated by silica precipitation experiments. Chem Geol 397, 94-105.

Oelze, M., von Blanckenburg, F., Hoellen, D., Dietzel, M., Bouchez, J., 2014. Si stable isotope fractionation during adsorption and the competition between kinetic and equilibrium isotope fractionation: Implications for weathering systems. Chem Geol 380, 161-171.

Opfergelt, S., Delvaux, B., André, L., Cardinal, D., 2008. Plant silicon isotopic signature might reflect soil weathering degree. Biogeochemistry 91, 163-175

Olson, H.C., Drabon, N., Johnson D.T., 2022. Oxygen isotope insights into the Archean ocean and atmosphere. Biogeochemistry 91, 163-175. Earth Planet Sci Lett 591, 1-9

Pack, A., Herwartz, D., 2014. The triple oxygen isotope composition of the Earth mantle and understanding ΔO17 variations in terrestrial rocks and minerals. Earth Planet Sci Lett 390, 138-145

Pope, E.C., Bird, D.K., Rosing, M.T., 2012. Isotope composition and volume of Earth's early oceans. Proc Natl Acad Sci U S A 109, 4371-4376.

Pringle, E.A., Moynier, F., Savage, P.S., Badro, J., Barrat, J.-A., 2014. Silicon isotopes in angrites and volatile loss in planetesimals. Proc Natl Acad Sci U S A 111, 17029-17032

Rimstidt, J.D., Barnes, H., 1980. The kinetics of silica-water reactions. Geochim Cosmochim Acta 44, 1683-1699

Robert, F., Chaussidon, M., 2006. A palaeotemperature curve for the Precambrian oceans based on silicon isotopes in cherts. Nature 443, 969-972.

Roerdink, D.L., van den Boorn, S.H., Geilert, S., Vroon, P.Z., van Bergen, M.J., 2015. Experimental constraints on kinetic and equilibrium silicon isotope fractionation during the formation of non-biogenic chert deposits. Chem Geol 402, 40-51.

Savage, P.S., Georg, R.B., Williams, H.M., Halliday, A.N., 2013. The silicon isotope composition of the upper continental crust. Geochim Cosmochim Acta 109, 384-399.

Schopf, J.W., Klein, C., 1992. The Proterozoic biosphere: a multidisciplinary study. Cambridge University Press.

Sengupta, S., Pack, A., 2018. Triple oxygen isotope mass balance for the Earth's oceans with application to Archean cherts. Chem Geol 495, 18-26.

Sengupta, S., Peters, S.T., Reitner, J., Duda, J.-P., Pack, A., 2020. Triple oxygen isotopes of cherts through time. Chem Geol 554, 119789.

Sharp, Z., Gibbons, J., Maltsev, O., Atudorei, V., Pack, A., Sengupta, S., Shock, E., Knauth, L., 2016. A calibration of the triple oxygen isotope fractionation in the SiO2–H2O system and applications to natural samples. Geochim Cosmochim Acta 186, 105-119.

Siever, R., 1992. The silica cycle in the Precambrian. Geochim Cosmochim Acta 56, 3265-3272

Sugitani, K., 1992. Geochemical characteristics of Archean cherts and other sedimentary rocks in the Pilbara Block, Western Australia: evidence for Archean seawater enriched in hydrothermally-derived iron and silica. Precambrian Res 57, 21-47.

Sugitani, K., Yamamoto, K., Wada, H., Binu-Lal, S., Yoneshige, M., 2002. Geochemistry of Archean carbonaceous cherts deposited at immature island-arc setting in the Pilbara Block, Western Australia. Sediment Geol 151, 45-66.

Sugitani, K., Yamashita, F., Nagaoka, T., Yamamoto, K., Minami, M., Mimura, K., Suzuki, K., 2006. Geochemistry and sedimentary petrology of Archean clastic sedimentary rocks at Mt. Goldsworthy, Pilbara Craton, Western Australia: evidence for the early evolution of continental crust and hydrothermal alteration. Precambrian Res 147, 124-147.

Sun, Y., Wu, L., Li, X., Sun, L., Gao, J., Ding, T., 2016. Silicon isotope fractionation in rice and cucumber plants over a life cycle: Laboratory studies at different external silicon concentrations. Journal of Geophysical Research: Biogeosciences 121, 2829-2841.

Tartèse, R., Chaussidon, M., Gurenko, A., Delarue, F., Robert, F., 2017. Warm Archean oceans reconstructed from oxygen isotope composition of early-life remnants. Geochem Perspect Lett 3, 55-65

Taylor, S.R., McLennan, S., 1981. The composition and evolution of the continental crust: rare earth element evidence from sedimentary rocks. Philosophical Transactions of the Royal Society of London. Series A, Mathematical and Physical Sciences 301, 381-399.

Tréguer, P.J., Sutton, J.N., Brzezinski, M., Charette, M.A., Devries, T., Dutkiewicz, S., Ehlert, C., Hawkings, J., Leynaert, A., Liu, S.M., 2021. Reviews and syntheses: The biogeochemical cycle of silicon in the modern ocean. Biogeosciences 18, 1269-1289.

Trower, E.J., Fischer, W.W., 2019. Precambrian Si isotope mass balance, weathering, and the significance of the authigenic clay silica sink. Sediment Geol 384, 1-11

Van den Boorn, S., Van Bergen, M., Vroon, P., De Vries, S., Nijman, W., 2010. Silicon isotope and trace element constraints on the origin of~ 3.5 Ga cherts: implications for Early Archaean marine environments. Geochim Cosmochim Acta 74, 1077-1103.

Winter, B.L., Knauth, L.P., 1992. Stable isotope geochemistry of cherts and carbonates from the 2.0 Ga Gunflint Iron Formation: implications for the depositional setting, and the effects of diagenesis and metamorphism. Precambrian Res 59, 283-313.

Young, E.D., Galy, A., Nagahara, H., 2002. Kinetic and equilibrium mass-dependent isotope fractionation laws in nature and their geochemical and cosmochemical significance. Geochim Cosmochim Acta 66, 1095-1104

Zakharov, D.O., Marin-Carbonne, J., Alleon, J., Bindeman, I., 2021. Triple oxygen isotope trend recorded by Precambrian cherts: A perspective from combined bulk and in situ secondary ion probe measurements. Rev Mineral Geochem 86, 323-365.

Zheng, X.-Y., Beard, B.L., Reddy, T.R., Roden, E.E., Johnson, C.M., 2016. Abiologic silicon isotope fractionation between aqueous Si and Fe (III)–Si gel in simulated Archean seawater: Implications for Si isotope records in Precambrian sedimentary rocks. Geochim Cosmochim Acta 187, 102-122.